



## Modeling, Simulation and Extraction of Model Parameters of Dye-Sensitized Solar Cells (DSSCs) Using Different Single-Diode Models

J. B. Yerima<sup>1,a</sup>, Dunama William<sup>2</sup>, Alkali Babangida<sup>3</sup>, and S. C. Ezike<sup>1</sup>

<sup>1</sup>Department of Physics, Modibbo Adama University Yola, Nigeria

<sup>2</sup>Department of mathematics, Modibbo Adama University Yola, Nigeria

<sup>3</sup>Department of Science Education, COE Azare, Bauchi State, Nigeria

<sup>a</sup>bjyerima@gmail.com

**Abstract:** Modeling, simulation and extraction of model parameters of four DSSCs was carried out using four different models. The results show that model parameters depend on of the types of models and dyes (or DSSCs). Also, the fewer the number of model parameters the lesser the computation efforts and knowledge about the internal features of the photovoltaic system and vice versa. In addition, the photocurrent  $I_{ph}$  of a DSSC is constant for all models. Furthermore, the diode reverse saturation current  $I_o$  is inversely proportional to the absolute values of the series resistance  $R_s$  and shunt resistance  $R_{sh}$ . Moreover, the modified diode ideality factor depends on the number of model parameters and nature of dye/DSSC. However, models with higher number of model parameters (4 and 5) involving resistances manifest parameter irregularity. Nevertheless, the negative sign or complexity of the model parameters does not render them undesirable elements for researchers to use them in their application. Thus, the overall result shows that all the models used produced good I-V curve fit for all the solar cells studied irrespective of the presence of parameter irregularity.

**Keywords:** Modeling, simulation, model parameter, DSSCs, single diode model, parameter irregularity

### Introduction

Dye-sensitized solar cell (DSSC) is a type of solar cell made up of typical titanium dioxide  $TiO_2$  has attracted the most significant attention from many scientists and engineers for the recent decades after the work of [1]. The DSSC is well known as a green and inexpensive photovoltaic device due to its natural available abundant and simple fabrication compared to two other types of solar cells [2]. From the milestone finding, extensive studies were expanded on the theoretical as well as experimental to improve the efficiency from 7.1% to 13% from 1991 to 2014. The latter is a criterion for the commercial application [3]. The current experimental studies on DSSC, such as [4]-[6], were a focus on material manufacture.

The theoretical modeling of the previous works [7]-[9] may provide better information of how the system works. One of the theoretical modelings is the single-diode circuit model. A solid, single-junction PV cell that is not illuminated behaves very similarly to a semiconductor diode [10]. The conventional equation (1) describes a simple diode with a distinctive I-V curve.

$$I = I_o \left( e^{\frac{V}{a}} - 1 \right) \quad (1)$$

where the modified ideality diode factor (quality factor or emission coefficient) which varies with the nature of diode is determined according to the fabrication process and the semiconductor material.

When the semiconductor is illuminated, it will produce a photo-generated current  $I_{ph}$ , which will result in a vertical translation of the I-V curve of a quantity that is almost entirely related to the surface density of the incident energy.

Extraction of solar cell model parameters from valid experimental data or manufacturer's datasheet is important in the design, construction and performance evaluation of solar cells. Nevertheless, the theoretical application of manufacturer's datasets is usually preferred because it is less expensive and time saving but the technology to produce commercial DSSCs is still not yet developed. Consequently, the manufacturer's datasheets for DSSCs are not yet readily available in the market. Therefore, most often experimental data is used for modeling and simulation of DSSCs. It is against this background that experimental data for four DSSCs have been modeled and simulated based on the single-diode model. It is worth noting, all methods involving the diode model have one common drawback that current and voltage cannot be separated and hence it is not possible to obtain the exact analytical solutions of the transcendental or implicit current-voltage equation. This has been achieved using the properties of the Lambert W function [11]-[14], [16].

### A single-diode PV cell model

The equivalent circuit solar cell containing series resistance  $R_s$ , shunt resistance  $R_{sh}$ , photocurrent  $I_{ph}$ , diode saturation current  $I_o$ , modified diode ideality factor,  $a$  is depicted in Figure 1. The single-diode model.

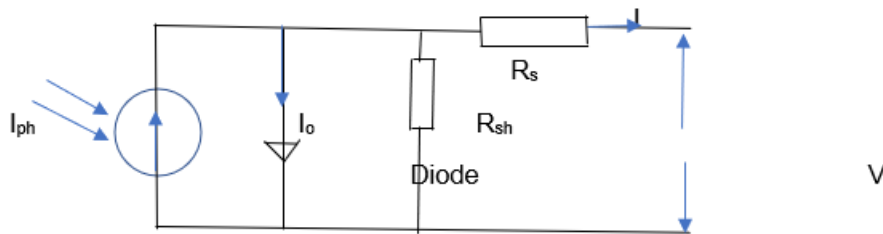


**Figure 1.** Electrical equivalent circuit of the single-diode solar cell

Assumes an ideal cell is pictured as a current generator that is linked to a parallel diode with an I-V characteristic which is mathematically defined by Schokley equation (2):

$$I = I_{ph} - I_o \left( e^{\frac{V+IR_s}{a}} - 1 \right) - \frac{V+IR_s}{R_{sh}} \quad (2)$$

Where  $I$  and  $V$  are the terminal current and voltage respectively,  $I_o$  the junction reverse current,  $a$  is the modified junction ideality factor,  $R_s$  and  $R_{sh}$  are the series and shunt resistance respectively. Equation (2) is transcendental in nature hence it is not possible to solve for  $V$  in terms of  $I$  and vice versa. However, explicit solutions can be obtained using the principal branch of the Lambert W-function  $W_0$  [11]-[14].

$$I = \frac{R_{sh}(I_{ph}+I_o)-V}{R_{sh}+R_s} - \frac{a}{R_s} W_o \left( \frac{R_{sh}R_s I_o}{a(R_{sh}+R_s)} e^{\left( \frac{R_{sh}R_s(I_{ph}+I_o)+VR_{sh}}{a(R_{sh}+R_s)} \right)} \right) \quad (3)$$

$$V = R_{sh}(I_{ph} + I_o) - (R_s+R_{sh})I - aW_o \left\{ \frac{R_{sh}I_o}{a} e^{R_{sh}\left(\frac{I_{ph}+I_o-I}{a}\right)} \right\} \quad (4)$$

One can directly find the current for a given value of voltage using equation (3) or the voltage via (4), which makes the computation easy and robust, in contrast to (2). The Lambert  $W$  function is readily available in all computation procedures [12]. Finally, for simulation purpose the current can be calculated for each model by plugging the appropriate model parameters for any given value of  $V$  into equation (3) and vice versa for for  $V$  any given value of  $I$  in equation (4).

Table 1. Principal characteristics of the 4 non-iterative parameter extraction methods

Method	Year	Number of parameters	Input data	Model parameters	Reference
El Tayyan	2009	2	$I_{sc}, V_{oc}, I_{mp}, V_{mp}$	$a, I_o$	
Saloux	2011	3	$I_{sc}, V_{oc}, I_{mp}, V_{mp}$	$a, I_{ph}, I_o$	
Aldwane	2014	4	$I_{sc}, V_{oc}, I_{mp}, V_{mp}$	$a, I_{ph}, I_o, R_s$	
Hejri	2016	5	$I_{sc}, V_{oc}, I_{mp}, V_{mp}$	$A, I_{ph}, I_o, R_s, R_{sh}$	

## The model equations

### 1. The El-Tayyan model [15]

The proposed El-Tayyan model for generating I-V characteristics of solar cell or PV module is in the form

$$I = I_{sc} - C_1 e^{\left(\frac{-V_{oc}}{C_2}\right)} \left( e^{\left(\frac{V}{C_2}\right)} - 1 \right) \quad (5)$$

where  $C_1$  and  $C_2$  are coefficients of the model equation. These coefficients are given by [16] as

$$C_1 = \frac{I_{sc}}{1 - e^{\left(\frac{-V_{oc}}{C_2}\right)}} \quad (6)$$

and, if  $V_{oc}/C_2 \gg 1$ :

$$C_2 = \frac{V_{mp} - V_{oc}}{W_{-1} \left( \left( 1 - \frac{V_{oc}}{V_{mp}} \right) \left( \frac{I_{mp}}{I_{sc}} \right) \right)} \quad (7)$$

However, [22], have shown that the relationships between the conventional model parameters ( $I_o$  and  $a$ ) and the El-Tayyan coefficients ( $C_1, C_2$ ) are given by equations (8) and (9)

$$I_o = C_1 e^{-\frac{V_{oc}}{C_2}} \quad (8)$$

$$a = C_2 \quad (9)$$

Thus,  $a$  and  $I_o$  in equations (8) and (9) are the two model parameters for the El-Tayyan model.

### II. The Saloux model [18]

An explicit photovoltaic (PV) model in terms of the ideal single-diode equivalent (no resistances) is reported in [18]. They derived some equations to calculate the three parameters at STC, but it appears that they are applicable to other conditions as well as slightly manipulated in equations (10-12).

$$a = \frac{V_{mp} - V_{oc}}{\ln\left(1 - \frac{I_{mp}}{I_{sc}}\right)} \quad (10)$$

$$I_{ph} = I_{sc} \quad (11)$$

$$I_o = \frac{I_{sc}}{e^{\frac{V_{oc}}{a} - 1}} \quad (12)$$

### III. The Aldwane model [19]

This is a four-parameter model ( $R_{sh}$  is neglected), which is very similar to Sera's method [20] except for a small difference in  $a$ : The remaining parameters  $I_{ph}$ ,  $I_o$ , and  $R_s$  are found via the exact same Sera's equations (14), (15) and (16) respectively.

$$a = \frac{2V_{mp} - V_{oc}}{\ln\left(\frac{I_{sc} - I_{mp}}{I_{sc}}\right) + \frac{I_{sc}}{I_{sc} - I_{mp}}} \quad (13)$$

$$I_{ph} = I_{sc} \quad (14)$$

$$I_o = I_{sc} e^{-\frac{V_{oc}}{a}} \quad (15)$$

$$R_s = \frac{a \ln\left(\frac{I_{sc} - I_{mp}}{I_{sc}}\right) + V_{oc} - V_{mp}}{I_{mp}} \quad (16)$$

### IV. The Hejri model [21]

The main purpose of the Hejri method is to approximate the five parameters to be used as initial values in a numerical solution algorithm. First  $a$  is found via Sera's (17), then  $I_{ph}$ ,  $R_s$  and  $R_{sh}$  by equations (18), (19) and (20) respectively.

$$a = \frac{2V_{mp} - V_{oc}}{\ln\left(\frac{I_{sc} - I_{mp}}{I_{sc}}\right) + \frac{I_{mp}}{I_{sc} - I_{mp}}} \quad (17)$$

$$I_{ph} = I_{sc} \quad (18)$$

$$R_s = \frac{V_{mp}}{I_{mp}} - \frac{\frac{2V_{mp} - V_{oc}}{I_{sc} - I_{mp}}}{\ln\left(\frac{I_{sc} - I_{mp}}{I_{sc}}\right) + \frac{I_{mp}}{I_{sc} - I_{mp}}} \quad (19)$$

$$R_{sh} = \sqrt{\frac{R_s}{\frac{I_{sc}}{a} e^{\left(\frac{R_s I_{sc} - V_{oc}}{a}\right)}}} \quad (20)$$

It is worth noting that equations (6-20) were used to calculate the appropriate model parameters whereas equations (3), (4) and (5) for the simulation of I-V and P-V curves for each of the models and DSSCs considered in this work. In this paper, the experimental results [17] partly reported in [22]-[23] were used to determine the model parameters of four DSSCs using four different models.

## Results And Discussion

Table 2. Source of natural dye and model parameters extracted from four solar cell models

Natural source of dye		El-Tayyan two-model parameters			
English Name (Scientific Name)	<i>a</i>	<i>I<sub>o</sub></i> (A)	<i>I<sub>ph</sub></i> (mA)	<i>R<sub>s</sub></i> (Ohm)	<i>R<sub>sh</sub></i> (Ohm)
Control (TiO <sub>2</sub> /N719)	0.195796	4.833×10 <sup>-4</sup>	-	-	-
Bitter gourd (Momordica charantia)	0.060393	1.293×10 <sup>-6</sup>	-	-	-
Bougainvillea (Bougainvillea)	0.229684	4.775×10 <sup>-4</sup>	-	-	-
Mango peel (Mongifera indica)	0.257501	2.504×10 <sup>-4</sup>	-	-	-
Natural source of dye		Saloux three-model parameters			
English Name (Scientific Name)	<i>a</i>	<i>I<sub>o</sub></i> (A)	<i>I<sub>ph</sub></i> (mA)	<i>R<sub>s</sub></i> (Ohm)	<i>R<sub>sh</sub></i> (Ohm)
Control (TiO <sub>2</sub> /N719)	0.114388	5.411×10 <sup>-5</sup>	9.355	-	-
Bitter gourd (Momordica charantia)	0.114176	8.532×10 <sup>-5</sup>	9.244	-	-
Bougainvillea (Bougainvillea)	0.111967	4.638×10 <sup>-5</sup>	3.450	-	-
Mango peel (Mongifera indica)	0.115474	1.195×10 <sup>-5</sup>	2.510	-	-
Natural source of dye		Aldwane four-model parameters			
English Name (Scientific Name)	<i>a</i>	<i>I<sub>o</sub></i> (A)	<i>I<sub>ph</sub></i> (mA)	<i>R<sub>s</sub></i> (Ohm)	<i>R<sub>sh</sub></i> (Ohm)
Control (TiO <sub>2</sub> /N719)	0.05843	3.85363×10 <sup>-7</sup>	9.355	12.3	-
Bitter gourd (Momordica charantia)	0.12570	1.3015×10 <sup>-4</sup>	9.244	-2.1	-
Bougainvillea (Bougainvillea)	0.03287	1.3898×10 <sup>-9</sup>	3.450	46.7	-
Mango peel (Mongifera indica)	0.03858	2.7731×10 <sup>-10</sup>	2.510	68.2	-
Natural source of dye		Hejri five-model parameters			
English Name (Scientific Name)	<i>a</i>	<i>I<sub>o</sub></i> (A)	<i>I<sub>ph</sub></i> (mA)	<i>R<sub>s</sub></i> (Ohm)	<i>R<sub>sh</sub></i> (Ohm)
Control (TiO <sub>2</sub> /N719)	0.080958	6.398×10 <sup>-6</sup>	9.355	7.4	199.5
Bitter gourd (Momordica charantia)	0.240064	9.913×10 <sup>-4</sup>	9.244	-23.3	117.7i
Bougainvillea (Bougainvillea)	0.045867	9.016×10 <sup>-8</sup>	3.450	39.0	1026.7
Mango peel (Mongifera indica)	0.048959	8.273×10 <sup>-9</sup>	2.510	59.0	4121.3



In Table 2 the source of natural dyes and the model parameters calculated from different models via equations (6-20) are included. The models considered include El Tayyan 2-parameter model, Saloux 3-parameter model, Aldwane 4-parameter model and Hejri 5-parameter model.

The El Tayyan model is a two-parameter model with the model parameters identified as the modified diode ideality factor  $a$  and the diode saturation current  $I_o$ . The results show that the magnitudes of both  $a$  and  $I_o$  depend on the natural dye in the ranges  $0.060393 \leq a \leq 0.257501$  and  $1.293 \times 10^{-6} \leq I_o \leq 4.833 \times 10^{-4}$  A respectively. The advantage of this model over the other existing models is that it doesn't require the knowledge of internal photovoltaic system parameters and involve less calculation efforts.

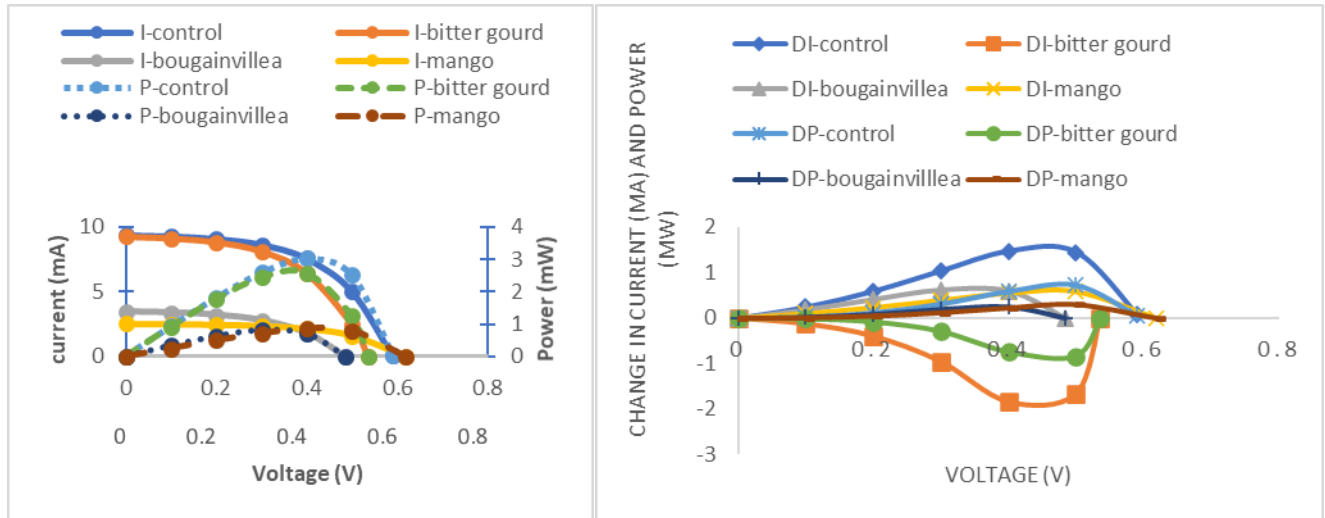
The Saloux model is a three-parameter model with the model parameters include the photocurrent  $I_{ph}$  in addition to the two mentioned under El Tayyan model. Also, the values of the model parameters vary moderately with the natural dyes in the ranges  $0.111967 \leq a \leq 0.115474$ ,  $1.195 \times 10^{-5} \leq I_o \leq 8.532 \times 10^{-5}$  and  $2.51 \leq I_{ph} \leq 9.355$  mA. Here, each of the model parameters for all dyes vary moderately in the same order such as  $a$  of order  $10^{-1}$ ,  $I_o$  of order  $10^{-5}$  and  $I_{ph}$  of order  $10^{-3}$ .

The Aldwane is a four-parameter model with model parameters namely series resistance  $R_s$  in addition to the three mentioned in Saloux model. Similarly, all the model parameters are functions of the natural dyes and they vary in the ranges  $0.03287 \leq a \leq 0.12570$ ,  $2.7731 \times 10^{-10} \leq I_o \leq 1.3015 \times 10^{-4}$  A,  $2.510 \leq I_{ph} \leq 9.355$  mA, and  $-2.1 \leq R_s \leq 68.2$  W. Also, each of the parameters vary in the order of ranges:  $a \sim 10^{-1}$ - $10^{-2}$ ,  $I_o \sim 10^{-10}$ - $10^{-4}$ ,  $I_{ph} \sim 10^{-3}$  and  $R_s \sim 10^1$ . Here, one of the values of  $R_s$  is observed to be negative, representing a case of parameter irregularity. Furthermore,  $I_o$  varies inversely proportional to  $R_s$ .

The Hejri model is a five-parameters model with shunt resistance  $R_{sh}$  in addition to the four mentioned in Aldwane model. Similarly, all the model parameters are functions of the natural dyes and they vary in the ranges  $0.045867 \leq a \leq 0.240064$ ,  $8.2731 \times 10^{-9} \leq I_o \leq 9.913 \times 10^{-4}$  A,  $2.510 \leq I_{ph} \leq 9.355$  mA,  $-2.1 \leq R_s \leq 68.2$  W and  $117.7i \leq R_{sh} \leq 4121.3$  W. In this case, one negative value of  $R_s$  is observed corresponding to one complex value of  $R_{sh}$ . Thus,  $R_s$  and  $R_{sh}$  are considered irregular parameters. Also,  $I_o$  varies inversely proportional to the absolute values of  $R_s$  and  $R_{sh}$ . The overall result shows that DSSC with bitter gourd dye has the maximum  $I_o = 9.913 \times 10^{-4}$  A and minimum  $R_s = -23.3$  W (or complex  $R_{sh} = 117.7i$ ) for the five-parameter model while DSSC with mango dye has the least  $I_o = 2.773 \times 10^{-10}$  A and maximum  $R_s = 68.2$  W for the four-parameter model.

In general, for all models  $I_{ph}$  for each DSSC remains constant. It is crystal clear that a model with lesser number of model parameters involves less computation efforts but lacks knowledge about the internal photovoltaic system parameters. However, on the other hand, a model with larger number of model parameters requires larger computation efforts and more knowledge about the photovoltaic system parameters is revealed. In this paper, only the 4- and 5-parameter models revealed parameter irregularity based on the sign of  $R_s$  or complexity of  $R_{sh}$ . Finally, computations using these models were extended to generate the I-V curves (Figure 2a) and the differences between measured and calculated currents (Figure 2b) for the solar cells in question.





(a)

(b)

**Figure 2.** (a) depicts the I-V and P-V curves of best fit with errors taken into account and (b) represents the distribution of the errors. All the models produced good curve fit even where the solar cell  $R_s$  has negative value and  $R_{sh}$  complex value which implies that the sign of the model parameters does not render them undesirable feature but researchers can still find them useful in their research work.

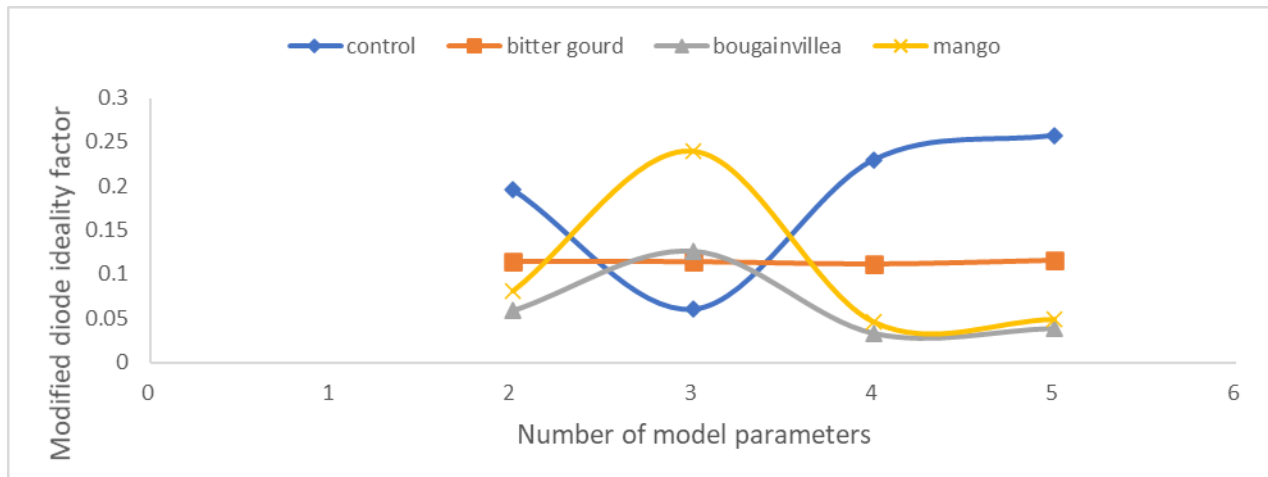


**Figure 3.** Dependence modified diode ideality factor on the type of model

Figure 3 depicts the dependence of the modified diode ideality factor of various DSSCs with different models. The variation of the modified diode ideality factor,  $a$ , for DSSC with bitter gourd dye with number of model parameters is very slowly or fairly constant to two decimal places (Table 2) representing a straight line parallel to the horizontal axis. But the variations of  $a$  with model type for the other DSSCs are nonlinear such that DSSCs with bougainvillea and mango dyes have maximum values of  $a$  for the 3-parameter model as opposed to the control DSSC with



minimum value of  $a$ . However, for further improvement, experiments with higher models like two-diodes, three-diodes, etc. and many equivalent resistances are required.

## Conclusions

In this study, modeling, simulation and extraction of model parameters of four DSSCs was performed using four different models. The major conclusions resulting from this work are:

1. The model parameters are dependent on the types of models and dyes/DSSCs
2. The fewer the number of model parameters the lesser the computation efforts and knowledge about the internal nature of the photovoltaic system and vice versa
3. The photocurrent  $I_{ph}$  of a DSSC/dye is constant for all models
4. The diode saturation current  $I_o$  is inversely proportional to the absolute values of the series resistance  $R_s$  and shunt resistance  $R_{sh}$
5. The modified diode ideality factor depends on the number of model parameters and dyes/DSSCs
6. Models with higher number of model parameters (4 & 5) involving resistances manifest parameter irregularity
7. The negative sign or complexity of the model parameters does not render them undesirable elements for researchers to use them in their application
8. All models provided good I-V curve fit for all DSSCs irrespective of the presence of parameter irregularity.

## References

- [1] O'Regan B. and Gratzel M., 1991, A low-cost, high efficiency solar cell based on dye-sensitized colloidal  $TiO_2$  films, *Nature*, vol. 353, page 737-740.
- [2] Gong J, Sumathy K, Qiao Q, and Zhou, 2017, Review on dye-sensitized solar cells (DSSCs) Advanced techniques and research trends *Renew, Sustainable Energy Rev.*, vol. 68, pp. 234-46.
- [3] Mathew S, Yella A, Gao P, Humphry-Baker R, Curchod B F E, Ashari-Astani N, Tavernelli I, Rothlisberger U, Nazeeruddin M K, and Gratzel M, 2014, Dye-sensitized solar cells with 13% efficiency achieved through the molecular engineering of porphyrin sensitizers, *Nat. Chem.*, vol. 6, pp. 242.
- [4] Yang R, Cai J, Lv K, Wu X, Wang W, Xu Z, Li M, Li Q and Xu W, 2017, Fabrication of  $TiO_2$  hollow microspheres assembly from nanosheets ( $TiO_2$ -HMS8-NS8) with enhanced photoelectric conversion efficiency in DSSCs and photocatalytic activity, *Appl. Catal. B Environ.*, vol. 2210, pp. 184-193.





- [5] Kazmi S A, Hameed S, Ahmed A S, Arshad M, and Azam A, 2017, Electrical and optical properties of graphene-TiO<sub>2</sub> nanocomposite and its applications in dye-sensitized solar cells (DSSCs), *J. Alloys Compd.*, vol. 691, pp. 659-665.
- [6] Kundu S, Sarojinijeeva P, Karthick R, Anantharaj G, Saritha G, Bera R, Anandnan S, Patra A, Ragupathy P, Selvaraj M, Jeyakumar D and Pillai K V, 2017, Enhancing the efficiency of DSSCs by the modification of TiO<sub>2</sub> photoanodes using N, F and S, co-doped graphene quantum dots, *Electrochimica Acta*, vol. 242, pp. 337-343.
- [7] Wang, Y., Wu, D., Fu, L. M., Ai, X. C., Xu, D., & Zhang, J. P., 2014, Density of state determination of two types of intra-gap traps in dye-sensitized solar cells and its influence on device performance, *Physical Chemistry Chemical Physics*, vol 16(23), pp. 11626-11632.
- [8] Hsiao, P. T., Tung, Y. L., & Teng, H., 2010, Electron transport patterns in TiO<sub>2</sub> nanocrystalline films of dye-sensitized solar cells, *The Journal of Physical Chemistry C*, vol. 114(14), pp. 6762-6769.
- [9] Villanueva-Cab, J., Jang, S. R., Halverson, A. F., Zhu, K., & Frank, A. J. (2014). Trap-free transport in ordered and disordered TiO<sub>2</sub> nanostructures. *Nano letters*, 14(5), pp. 2305-2309.
- [10] Humada, A. M., Hojabri, M., Mekhilef, S., & Hamada, H. M., 2016, Solar cell parameters extraction based on single and double-diode models: A review, *Renewable and Sustainable Energy Reviews*, vol. 56, pp. 494-509.
- [11] Batzelis, E. I., & Papathanassiou, S. A., 2015, A method for the analytical extraction of the single-diode PV model parameters, *IEEE Transactions on Sustainable Energy*, vol. 7(2), pp. 504-512.
- [12] Cubas, J., Pindado, S., & De Manuel, C., 2014, Explicit expressions for solar panel equivalent circuit parameters based on analytical formulation and the Lambert W-function, *Energies*, 7(7), pp. 4098-4115.
- [13] Petrone, G., Ramos-Paja, C. A., & Spagnuolo, G., 2017, Photovoltaic sources modeling, *John Wiley & Sons.*, pp. 208.
- [14] Mahmoud, Y., & El-Saadany, E. F., 2015, Fast power-peaks estimator for partially shaded PV systems, *IEEE Transactions on Energy Conversion*, vol. 31(1), pp. 206-217.
- [15] El Tayyan, A., 2006, An Empirical model for generating the IV Characteristics for a Photovoltaic System, *Al-Aqsa University Journal (Natural Sciences Series)*, vol 10, pp. 214-221.
- [16] Roibás-Millán, E., Cubero-Estalrich, J. L., Gonzalez-Estrada, A., Jado-Puente, R., Sanabria-Pinzon, M., Alfonso-Corcuera, D., & Pindado, S., 2020, Lambert W-function simplified expressions for photovoltaic current-voltage modelling, *IEEE*



- 
- International Conference on Environment and Electrical Engineering and 2020 IEEE Industrial and Commercial Power Systems Europe (EEEIC/I&CPS Europe)*, pp. 1-6.
- [17] Babangida A., 2022, A study of the absorbance, stability and storage temperature of organic dyes for an enhanced performance of dye-sensitized solar cells. *PhD Dissertition Modibbo Adama Uni. Yola, Nigeria*.
- [18] Saloux, E.; Teyssedou, A.; Sorin, M., 2011, Eplicit model of photovoltaic panels to determine voltages and currents at the maximum power point. *Sol. Energy*, vol. 85, pp. 713-722.
- [19] Aldwane, B., 2014, Modeling, simulation and parameters estimation for Photovoltaic module, *In 2014 First International Conference on Green Energy ICGE 2014*, pp. 101-106.
- [20] Sera, D., Teodorescu, R., & Rodriguez, P., 2008, Photovoltaic module diagnostics by series resistance monitoring and temperature and rated power estimation. *In 2008 34th annual conference of IEEE industrial electronics*, pp. 2195-2199.
- [21] Hejri, M., Mokhtari, H., Azizian, M. R., Ghandhari, M., & Söder, L., 2014, On the parameter extraction of a five-parameter double-diode model of photovoltaic cells and modules, *IEEE Journal of Photovoltaics*, vol. 4(3), pp. 915-923.
- [22] Babangida, A., Yerima, J. B., Ahmed, A. D., & Ezike, S. C., 2022, Strategy to select and grade efficient dyes for enhanced photo-absorption, *African scientific reports*, pp. 16-22.
- [23] Yerima, J. B., Babangida, A., Ezike, S. C., Dunama, W., & Ahmed, A. D., 2022, Matrix Method of Determining Optical Energy Bandgap of Natural Dye Extracts, *Journal of Applied Sciences and Environmental Management*, vol. 26(5), pp. 943-948.